

Isolated Two-Inductor Boost Converter with One Magnetic Core

Liang Yan Brad Lehman
 Department of Electrical and Computer Engineering
 Northeastern University
 Boston, MA 02115

Abstract- This paper presents a new isolated two-inductor boost converter. All magnetic components are integrated into one magnetic core. The circuit has the two inductor windings intrinsically coupled. The operation principle of the new circuit is presented. A prototype 100W DC/DC boost converter has been built. Experimental and simulation results are both presented.

I. INTRODUCTION

The two-inductor boost converter exhibits many advantages in high power, low input voltage to high output voltage conversion applications [1-5]. Large input current can be split between the two inductors on the primary side. This effectively reduces the current stress in the circuit. The two primary switches have low conduction loss, and the driving circuit is simple [2]. The converter can be implemented as either non-isolated or isolated formats. An isolated two-inductor boost converter is shown in Fig. 1.

The main problem of this circuit is the limited output voltage regulation range when duty ratio is small [3]. Even when the overlapping between the driving pulses of the two primary switches is close to zero, the two inductors L_1 and L_2 are always charged, no matter what the load is. Fig. 2 shows the condition when the input power is minimum, i.e. both primary switches have minimum duty ratio 0.5 and the current in each inductor is critically continuous. The positive and negative voltage pulses on each inductor have the same amplitude and duration. Then, the minimum average input power is $V_i^2 T / 2L$, where L is the inductance of each inductor; V_i is the input voltage; T is the switching period. If the load is below the minimum input power, further decreasing the load will cause the output voltage to increase abnormally because of the excessive energy storage in the inductors. The desired character is to keep the input power close to zero even when the driving pulses have overlap close to zero.

One solution is given in Fig. 3 [3]. An auxiliary transformer T_2 is in series with the two inductors L_1 and L_2 . Essentially, this transformer magnetically couples the two input current paths. As a result, the currents in the two inductors are always the same. Ideally, this eliminates the inductor currents when the load is close to zero. It makes discontinuous inductor current possible. In this circuit, four magnetic components are used. To reduce the number of the magnetic components, the integration of the two inductors with the auxiliary transformer

is introduced. However, in the isolated format, the isolation transformer is always needed.

This paper proposes a new integrated magnetic isolated two-inductor boost converter that uses only one magnetic component. Specifically, the new circuit

- implements the isolated two-inductor boost converter with one transformer.
- has two inductor windings intrinsically coupled. Under the condition that the output voltage is regulated, the input power is limited when the overlapping period of the two switches is close to zero.
- can be implemented with one gap in a three-leg magnetic core.

Section II presents the proposed new two-inductor boost converter and its operating principle. Section III shows the transformer design procedure. Section IV discusses some practical issues in implementation. Section V presents simulation and experimental results. Section VI gives conclusions.

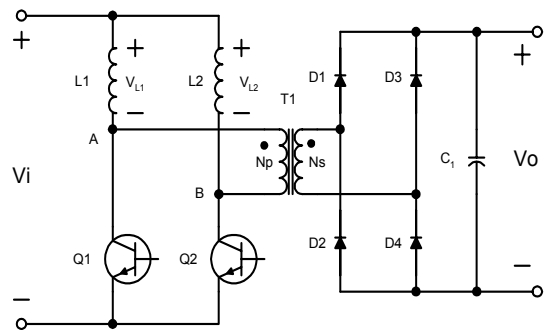


Fig. 1 Conventional Two-Inductor Boost Converter

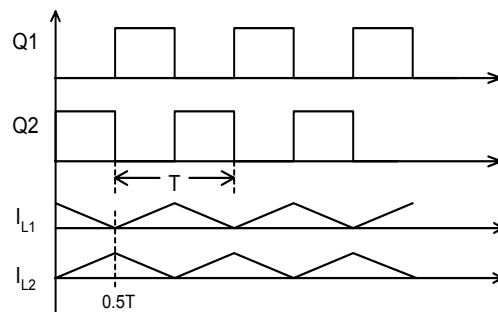


Fig. 2 Minimum Load Condition

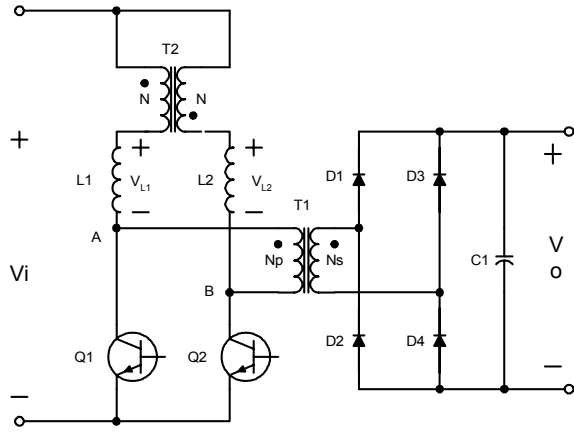


Fig. 3 Two-Inductor Boost Converter with Auxiliary Transformer [3]

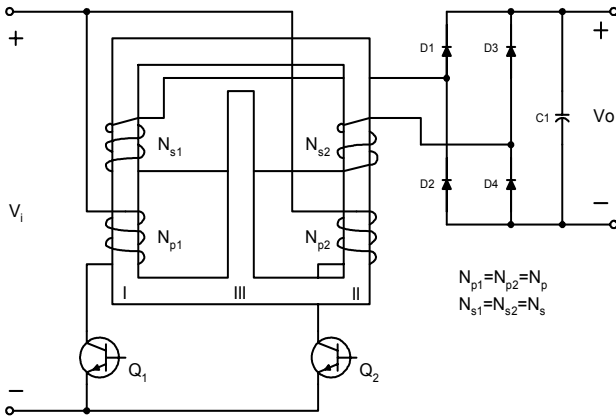


Fig. 4 Proposed Integrated Magnetic Two-Inductor Boost Converter

II. THE PROPOSED INTEGRATED MAGNETIC TWO-INDUCTOR BOOST CONVERTER

Fig. 4 is the proposed integrated magnetic two-inductor boost converter. The transformer uses a single three-leg magnetic core with a gap in the center leg. Two inductor windings N_{p1} and N_{p2} are wound on the two outer legs. Secondary windings N_{s1} and N_{s2} are wound on the two outer legs respectively and connected in series. Since N_{p1} and N_{p2} are on the primary side and behave as primary windings in part of switching cycle, we refer to them in this paper as primary windings.

Fig. 5 illustrates the operating waveforms of the proposed two-inductor boost converter. Time $t_1 \sim t_5$ shows four operating phases in one switching cycle. Fig. 6 shows the capacitive models for operating phases $t_1 \sim t_2$ and $t_2 \sim t_3$ [6,7]. The operating phases $t_3 \sim t_4$ and $t_4 \sim t_5$ are similar. In this capacitive model, each current source or sink represents an active winding; $\dot{\Phi}$ is the flux rate (i.e. the derivative of flux) within

each leg; P is the permeance of the gap or each core leg; F is the magnetomotive force (MMF) on the permeance.

Fig. 7 shows the current flowing paths in each phase. To simplify the analysis, all the devices are assumed to be ideal. The magnetomotive forces on the permeances of the core legs are neglected, i.e. these permeances are assumed to be infinite compared with the permeance of the gap. Let the driving signals of Q_1 and Q_2 be as in Fig.5. The operation principle can be explained as following, referring to Fig. 7.

a. Time $t_1 \sim t_2$: At this time interval, both switches Q_1 and Q_2 conduct. The currents in the primary windings increase as I_{Np1} and I_{Np2} in Fig. 5. The induced voltages on the secondary windings N_{s1} and N_{s2} have opposite polarities. The overall voltage difference on the two output terminals of the secondary windings is zero. All diodes are blocked. The output voltage is held by the output capacitor. The flux level in the gap Φ_g increases. This is the energy storage stage as in a typical boost circuit.

The flux rates in the two outer legs can be determined directly from the voltages on the two primary windings N_{p1} and N_{p2} :

$$\dot{\Phi}_{p1} = \frac{V_i}{N_{p1}} \quad (1)$$

$$\dot{\Phi}_{p2} = \frac{V_i}{N_{p2}} \quad (2)$$

The flux rate in the center leg is the summation of the flux rates in the two outer legs, i.e.

$$\dot{\Phi}_{g_1} = \dot{\Phi}_{p1} + \dot{\Phi}_{p2} \quad (3)$$

Let $N_{p1} = N_{p2} = N_p$. Then from (1), (2) and (3), the flux rate in the center leg is

$$\dot{\Phi}_{g_1} = \frac{2V_i}{N_p} \quad (4)$$

b. Time $t_2 \sim t_3$: Switch Q_2 turns off. In this stage, N_{p1} continues receiving energy from the input and I_{Np1} increases. The induced voltages on secondary windings N_{s1} and N_{s2} force diodes D_2 and D_3 to conduct. The currents in D_2 and D_3 are as shown in Fig. 5 by $I_{D2/3}$. This current charges the output capacitor. The flux level in the gap (Φ_g) decreases.

Applying the same derivation method, the flux rate in the center leg is obtained:

$$\dot{\Phi}_{p1} = \frac{V_i}{N_{p1}} \quad (5)$$

$$\dot{\Phi}_{s2} = \frac{V_o - V_i N_{s1} / N_{p1}}{N_{s2}} \quad (6)$$

In this operating phase, the flux rate in the center leg is the difference of the flux rates in the two outer legs,

$$\dot{\Phi}_{g_2} = \dot{\Phi}_{s2} - \dot{\Phi}_{p1} \quad (7)$$

Leg $N_{s1} = N_{s2} = N_s$ From (5), (6) and (7),

$$\dot{\Phi}_{g-2} = \frac{V_o}{N_s} - \frac{2V_i}{N_p} \quad (8)$$

c. Time $t_3 \sim t_4$: Both switches Q_1 and Q_2 conduct. This operating phase is the same as that in time interval $t_1 \sim t_2$.

d. Time $t_4 \sim t_5$: Switch Q_1 turns off. In this phase, N_{p2} receives energy from the input, while N_{p1} is disconnected from the input. Diodes D_1 and D_4 conduct.

It is obvious that the flux change on the center leg must be balanced in a half cycle. Define duty ratio D and period T as in Fig. 5. Phase $t_1 \sim t_2$ has time duration $(D-0.5)T$. Phase $t_2 \sim t_3$ has time duration $(1-D)T$. Apply the flux balance equation on the gap:

$$(D-0.5)T \times \dot{\Phi}_{g-1} = (1-D)T \times \dot{\Phi}_{g-2} \quad (9)$$

From (4), (8) and (9), the output-to-input voltage transfer ratio is obtained:

$$\frac{V_o}{V_i} = \frac{N_s}{N_p} \frac{1}{1-D} \quad (10)$$

To derive the current relations, let I_{s1} , I_{s2} be the current in the secondary windings; I_{p1} and I_{p2} be the current in the primary windings; I_{in} be the input current; F_g be the magnetomotive force on the gap; F_i ($i = I-III$) be the magnetomotive force on the core legs. Assume that the magnetomotive forces on the core legs are neglected. Then, in Fig. 6, $F_I = F_{II} = F_{III} = 0$. In time duration $t_1 \sim t_2$,

$$F_{p1} = F_g \quad (11)$$

$$F_{p2} = F_g \quad (12)$$

From the definition of magnetomotive force,

$$F_{p1} = N_{p1} I_{p1} \quad (13)$$

$$F_{p2} = N_{p2} I_{p2} \quad (14)$$

The input current is the summation of the currents in the two primary windings,

$$I_{in} = I_{p1} + I_{p2} \quad (15)$$

From (11) to (15), $I_{in} = \frac{2F_g}{N_p}$ (16)

In time duration $t_2 \sim t_3$, for the same reason,

$$F_{p1} = F_g + F_{s1} \quad (17)$$

$$F_{s2} = F_g \quad (18)$$

$$I_{s1} = I_{s2} \quad (19)$$

From definition, $F_{s1} = N_{s1} I_{s1}$ (20)

$$F_{s2} = N_{s2} I_{s2} \quad (21)$$

$$F_{p1} = N_{p1} I_{p1} \quad (22)$$

The input current only goes through primary winding N_{p1} ,

$$I_{in} = I_{p1} \quad (23)$$

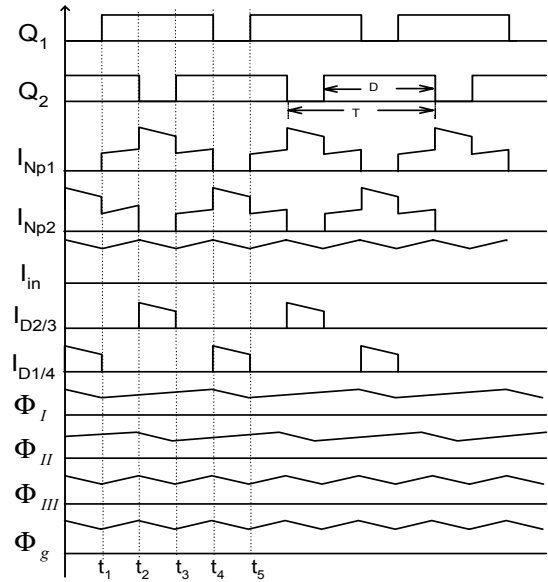
From (17) to (23),

$$I_{in} = \frac{2F_g}{N_p} \quad (24)$$

According to (16) and (24), the input current is always proportional to the magnetomotive force on the gap. Equation (4) and (8) indicate that the flux rate in the center leg is a constant in each phase. So the magnetomotive force on the gap (F_g) increases or decreases linearly. This causes the input current I_{in} to increase or decrease linearly as in Fig. 5.

To address the coupling between the two primary windings, assume the two driving signals have non-overlapping time interval. If the output voltage is kept high enough, when only one switch, for example, Q_1 turns on, the center leg exhibits large flux resistance to primary winding N_{p1} compared to the opposite outer leg, i.e. *Leg II*, because of the gap. Most flux rate goes through *Leg II*. The magnetomotive force on the gap F_g increases slowly. This implies that the input current increases slowly. From another point of view, since most flux rate goes through *Leg I* and *Leg II*, the transformer behaves as large inductance to the input source and limits the input current.

Note that the output voltage must be high enough, or, regulated. Otherwise, if the output voltage drops below the reflected input voltage, the transformer will transfer input energy directly to the secondary side. Some safety mechanism should be provided to turn off the switches from abnormal output voltage. This problem is further detailed in Section IV.



Q_1, Q_2 : the driving signals of two primary switches; I_{Np1} and I_{Np2} : the currents in the two primary windings; I_{in} : the input current; $I_{D1/4}$: the current in diode D_1 and D_4 ; $I_{D2/3}$: the current in diode D_2 and D_3 ; $\Phi_I \sim \Phi_{III}$: the flux in the core legs; Φ_g : the flux in the gap.

Fig.5 Operating Waveforms

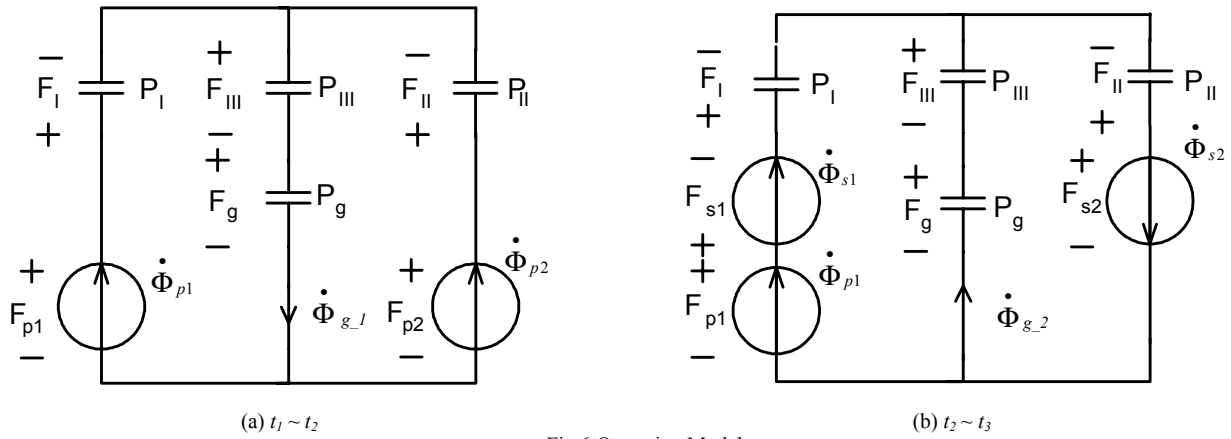


Fig.6 Operating Models

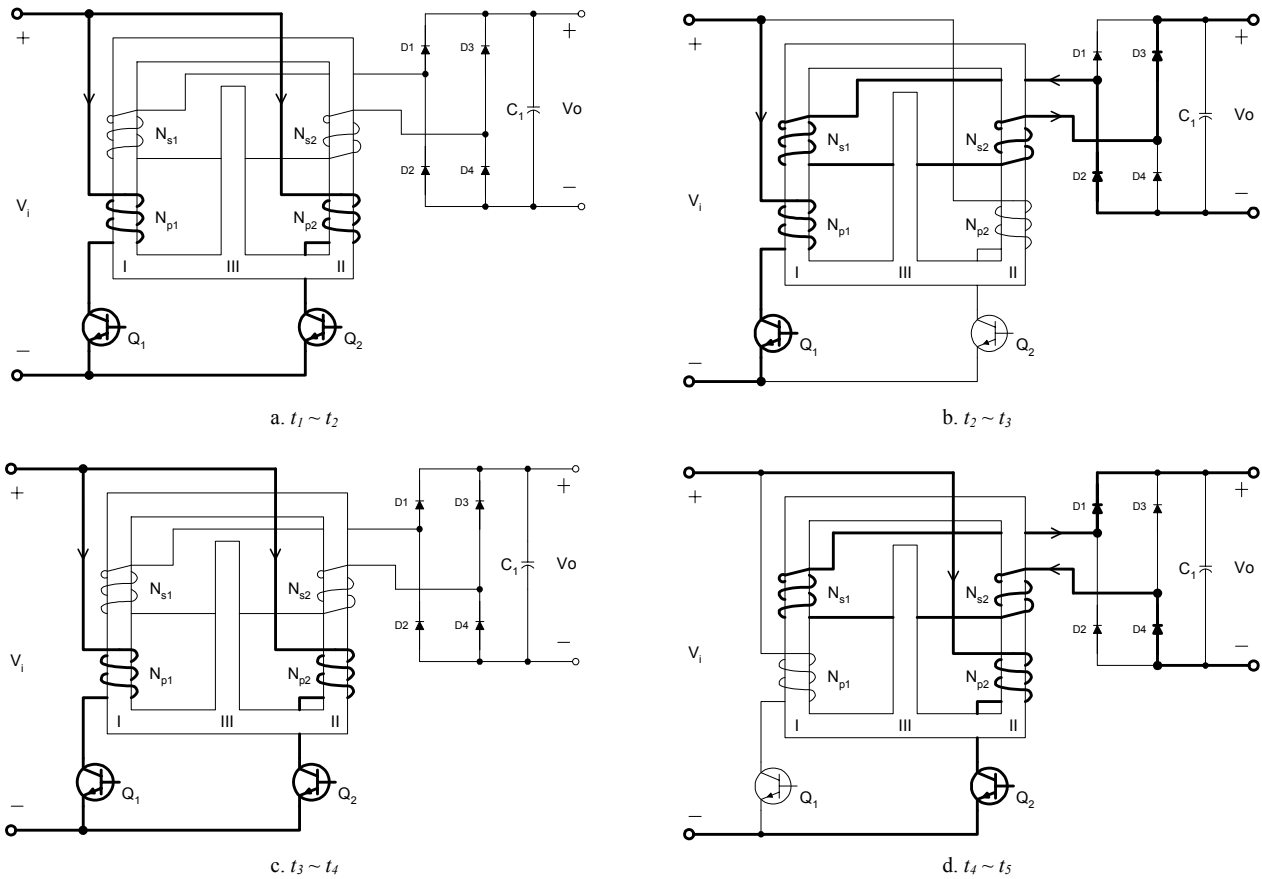


Fig.7 Current Paths

III. DESIGN PROCEDURE

The design philosophy here is to select the number of primary and secondary winding turns for a specified magnetic core to achieve tolerable input current ripple and peak flux densities in each core leg. Specifically, these parameters include

- Primary winding turn $N_{p1} = N_{p2} = N_p$;
- Secondary winding turn $N_{s1} = N_{s2} = N_s$;

Step 1: Select the secondary-to-primary winding turns ratio $n = N_s/N_p$.

The secondary-to-primary winding turns ratio is determined by the input and output voltage specification by using (10). Typically, n is selected to be as large as possible to use the duty ratio more efficiently and to reduce the number of primary winding turns. The maximum turn ratio is $0.5V_o/V_i$, which is limited by the minimum duty ratio 0.5.

Step 2: Select the winding turns.

N_p and N_s are determined by the input current ripple and the peak flux densities in each core leg. The following formulas can be used to verify that these results are within the tolerance.

1. Input current ripple.

The peak-to-peak input current ripple can be derived as

$$I_{in_d} = \frac{2V_o(2D-1)(1-D)}{N_p N_s f_s P_g} \quad (25)$$

P_g is the permeance of the gap, which is defined by $P_g = \mu_0 A/l_g$ and typically specified as A_L value in datasheet. f_s is the switching frequency. μ_0 is the permeability of air. A is the cross-sectional area of the gap. l_g is the gap length.

2. Peak flux density in the magnetic core.

The average flux density in the center leg is

$$B_{c_av} = \frac{N_p I_{in_av} P_g}{2A_c} \quad (26)$$

where I_{in_av} is the average input current; A_c is the cross-sectional area of the center leg.

The average flux density in the outer legs is (identical in the two outer legs)

$$B_{o_av} = B_{c_av}/2 \quad (27)$$

The flux swing in the center leg is

$$B_{c_d} = \frac{2V_o(1-D)(D-0.5)}{N_s f_s A_c} \quad (28)$$

The flux swing in the outer legs is

$$B_{o_d} = \frac{V_o D(1-D)}{N_s f_s A_o} \quad (29)$$

where A_o is the cross-sectional area of the outer legs.

The peak flux density in the center leg is

$$B_{c_p} = B_{c_av} + B_{c_d}/2 \quad (30)$$

The peak flux density in the outer legs is

$$B_{o_p} = B_{o_av} + B_{o_d}/2 \quad (31)$$

Both B_{c_p} and B_{o_p} must be below the saturation value.

IV. PRACTICAL CONSIDERATIONS

A. Start-up.

Before the circuit starts up, the output voltage is zero. If Q_1 and Q_2 begin to operate, the transformer-style coupling between the primary and secondary winding will transfer energy directly from the primary side to the secondary side without inductor filtering. This is illustrated in Fig. 8. Suppose Q_2 is off and Q_1 is on. Since the center leg exhibits large flux resistance to the primary winding N_{p1} , most flux will go through *Leg II*. The induced voltages on N_{s1} and N_{s2} have

the polarities as in Fig. 8. Both diodes D_2 and D_3 conduct. The resulting large initial current may damage the semiconductor devices in the current path. The output capacitor must be pre-charged in advance to block the diodes. The minimum charged voltage is derived as follows:

Let the maximum input voltage be denoted as V_{i_max} . If this voltage is applied on the primary winding, the induced voltage on the secondary windings should be less than the output voltage, i.e.

$$\frac{V_{i_max}}{N_p} \times 2N_s < V_o$$

or, the pre-charged voltage V_{o_pre} should satisfy

$$V_{o_pre} \geq 2 \frac{N_s}{N_p} V_{i_max} \quad (32)$$

B. Protection.

Even applying a protection mechanism in the control unit, occasional duty ratio error ($D < 0.5$) may occur. This will damage the converter because there is no path to release the energy in the gap when both switches turn off. One of the solutions is to add additional paths on the secondary side as in Fig. 9 and Fig.10. Fig. 9 shows the transformer with one additional winding N_{Ls} on the center leg. Fig. 10 shows the transformer with two additional windings N_{Ls1} and N_{Ls2} on the two outer legs respectively. When both primary switches turn off, these additional windings provide current paths to release the energy from the gap to the secondary side. However, these additional windings should only function when both switches turn off to avoid interfering the normal operation. As the following derivation shows, this places limit on the maximum duty ratio and the maximum winding turns.

Referring to the circuit in Fig. 9, in operation phase $t_1 \sim t_2$, the direction of flux rate in the center leg is downward as in Fig. 6. The induced voltage on the inductor winding blocks the diode D_5 . However, in operation time $t_2 \sim t_3$, the flux flow in the center leg has the temptation to forward bias the diode D_5 . To avoid this, the induced voltage on N_{Ls} must be less than the output voltage in such an operating condition.

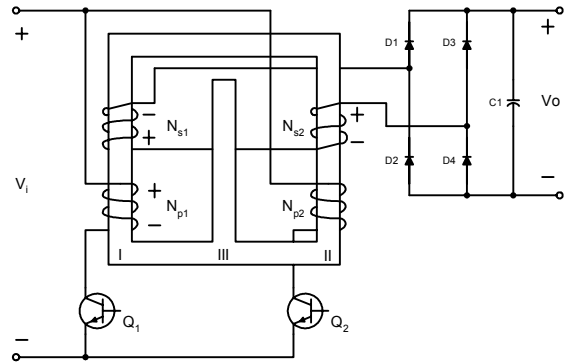


Fig. 8 Circuit Start-up

In operation phase $t_2 \sim t_3$, the flux rate in the center leg is given by (8). So

$$\left(\frac{V_o}{N_s} - \frac{2V_i}{N_p}\right) \times N_{Ls} < V_o \quad (33)$$

From (10) and (33), the inductor winding turn has the constraint

$$N_{Ls} < \frac{N_s}{2D-1} \quad (34)$$

For the same reason, the windings N_{Ls1} and N_{Ls2} in Fig. 10 should satisfy

$$N_{Ls1} < \frac{N_s}{D}, N_{Ls2} < \frac{N_s}{D} \quad (35)$$

If the number of the additional inductor winding turns is large, the current going through the winding is small. Since the inductor winding is used for occasional control fault and typically wound by thin wires, it is desirable to have many inductor winding turns. However, if the number of the inductor winding turns is too large, the maximum duty ratio becomes too small. This decreases the regulation range. The design of protection circuit must make trade-offs between these issues.

C. Control.

Boost converters typically exhibit a right half plane zero in its small signal model. This limits the bandwidth of the control loop. So, it is important to identify the position of the zero. The proposed integrated magnetic two-inductor boost converter has output voltage to control small signal transfer function:

$$\frac{\hat{v}_o}{\hat{d}} = \frac{-\frac{V_o}{RC(1-D)} \left[s - \frac{4R(1-D)^2}{N_s^2 P_g} \right]}{s^2 + \frac{1}{RC}s + \frac{4(1-D)^2}{N_s^2 P_g C}} \quad (36)$$

The right half plane zero is located at $\frac{4R(1-D)^2}{N_s^2 P_g}$, where R is the load resistance; C is the output capacitance.

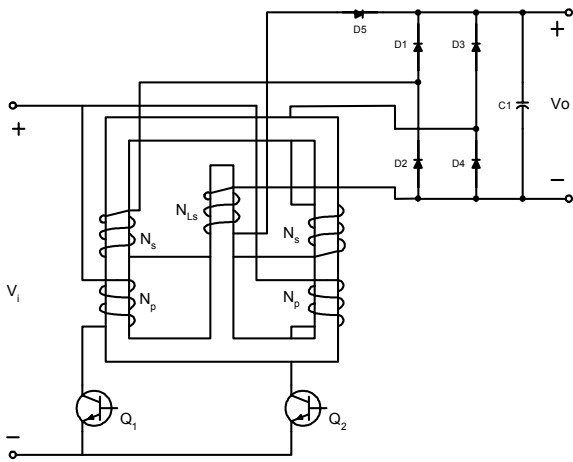


Fig. 9 Circuit with one Protection Winding

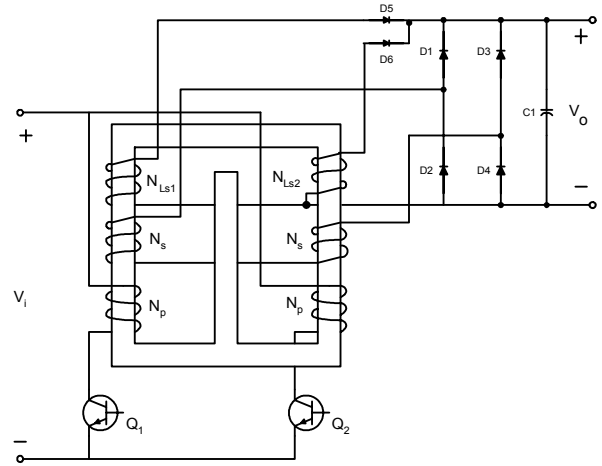


Fig. 10 Circuit with Two Protection Windings

V. EXPERIMENTAL AND SIMULATION RESULTS

An experimental integrated magnetic two-inductor boost converter was designed to verify the principles. Although this topology is better suited for high power application, the experiment was implemented on a 100W level (due to academic lab facility limitations.) The design specifications are:

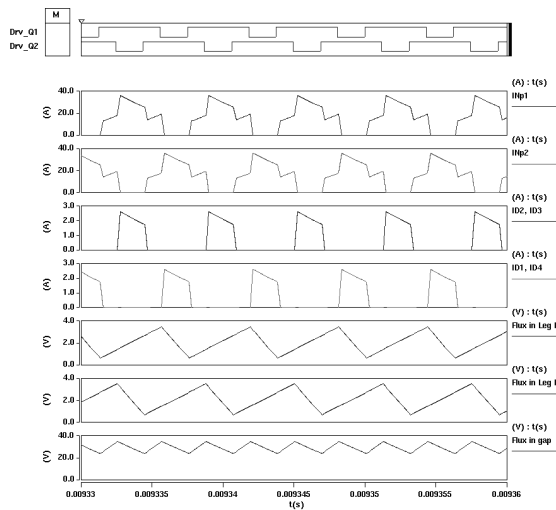
- Input Voltage: 3.3V;
- Output voltage: 72V;
- Maximum input current ripple 10A.

The maximum turn ratio is 10 because of the minimum duty ratio 0.5. According to the power level, an E22/6/3F3 magnetic core was selected for the transformer and switching frequency is set at 160kHz. From (25), 2 primary winding turns is minimum to satisfy input current ripple requirement. In this design, the secondary winding is selected to have 14 turns. The flux densities can be calculated as:

- Peak flux density in the center leg 157mT;
- Peak flux density in the outer legs 223mT.

Simulation results are shown in Fig. 11, where I_{Np1} and I_{Np2} are the currents in the two input inductors. I_{D1-4} are the currents in the output diodes. The fluxes in the legs are shown from their respective magnetomotive forces.

The experimental circuit is as in Fig. 9. The primary switches uses 3 paralleled Si4466. The secondary rectifiers are BYV200. The protection winding on the center leg has 18 winding turns. It only functions when the duty ratio is less than 0.5. Experimental results are shown in Fig. 12. to Fig. 14. Both have input 3.3V/11.2A and output 72V/0.45A. In Fig. 12, Channel 1 and Channel 2 are the driving signals. Channel 3 is the drain-source voltage waveform on primary switch Q_2 . Channel 4 shows the input current waveform, which is the addition of the currents in the two primary windings. In Fig. 13, Channel 4 shows the current in primary windings N_{p2} . In Fig. 14, Channel 3 is the output voltage. Channel 4 shows the current in output diode D_1 . Both the simulation and experimental results verify the operational principles of the circuit.



I_{Np1} , I_{Np2} : Inductor winding current; I_{D1-4} : Output diode current; Flux in Leg I, II and gap: Flux level (represented by MMF)

Fig. 11 Simulation Result

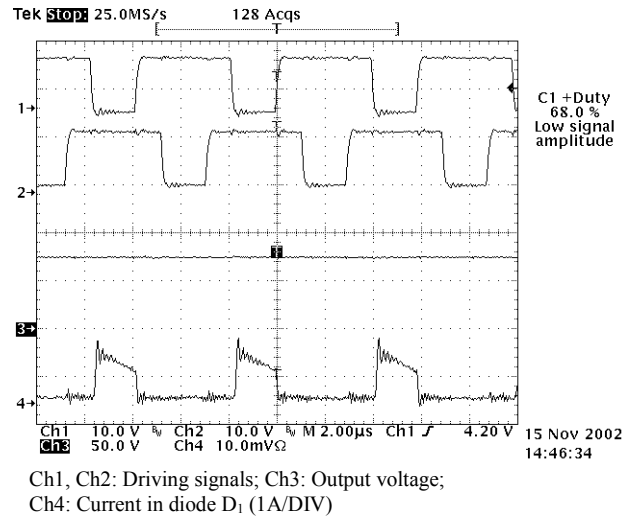


Fig. 14 Experimental Result

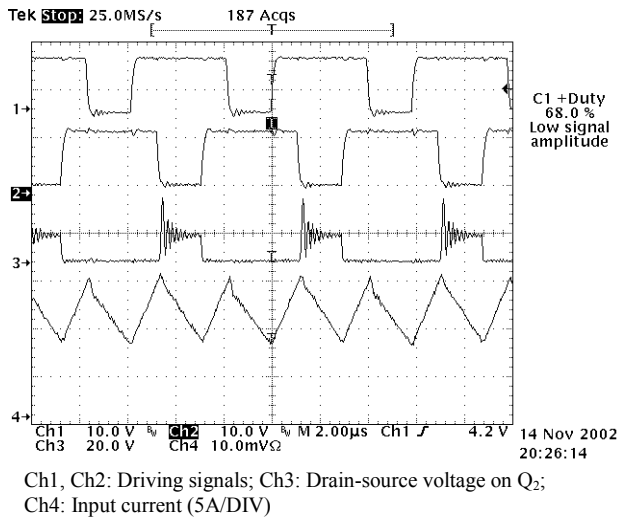


Fig. 12 Experimental Result

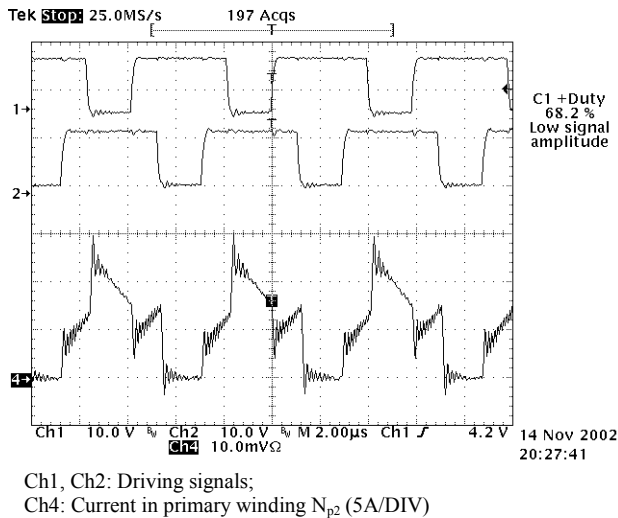


Fig. 13 Experimental Result

VI. CONCLUSION

A new integrated magnetic isolated two-inductor boost converter is presented. The new converter is implemented by using a single magnetic core with one gap in the center leg. The two inductor windings are intrinsically coupled. The operation principle is presented. Experimental and simulation results verify the new topology. Some practical considerations are discussed. The advantage of this topology is to reduce the magnetic components and at the same time keep the coupling between the two inductor windings. The limitation is that the coupling is only maintained when the output voltage is regulated. However, this condition is normally satisfied.

REFERENCE

- [1] M. S. Elmore "Input Current Ripple Cancellation in Synchronized, Parallel Connected Critically Continuous Boost Rectifier," *IEEE APEC*, pp. 152-158, 1996.
- [2] G. Ivensky, I. Elkin, S. Ben-Yakov, "An Isolated dc/dc Converter Using Two Zero Current Switched IGBT's in a Symmetrical Topology," *IEEE PESC*, pp. 1218-1225, 1994.
- [3] Y. Jang, M. M. Jovanovic, "New Two-inductor Boost Converter with Auxiliary Transformer," *IEEE APEC*, pp. 654-660, 2002.
- [4] Y. Jang, "Two-Inductor Boost Converter," *US Patent 6,239,584*, May 29, 2001.
- [5] P. J. Wolfs, "A Current-sourced dc-dc Converter Derived via the Duality Principle from the Half-bridge Converter", *IEEE Trans. On Industrial Electronics*, Vol. 40, No. 1, February 1993, pp. 139-144.
- [6] L. Yan, B. Lehman, "Better Understanding and Synthesis of Integrated Magnetics With Simplified Gyator Model Method," *IEEE PESC*, 2001.
- [7] D. C. Hamill, "Lumped Equivalent Circuits of Magnetic Components: The Gyator-Capacitor Approach," *IEEE Trans. On Power Electronics*, Vol. 8, No. 2, April 1993, pp. 97-103.